Water Air Soil Pollut (2020) 231:510
https://doi.org/10.1007/s11270-020-04890-7

Impact of Land Cover Changes on the Soil and Water Quality of Greens Bayou Watershed

Balaji Bhaskar Maruthi Sridhar · **Jericho Johnson** · **Adeola Mosuro**

Received: 14 June 2020 / Accepted: 24 September 2020

Abstract Rapid land use and land cover changes have a significant effect on ecology, environment, and human health in urban watersheds. With increase in frequency and intensity of the urban flooding events and repeated inundation of the neighborhoods, it is important to monitor the water and soil chemical characteristics in Greens Bayou Watershed (GBW) region. The objectives of this study were to (1) analyze the nutrient and heavy metal concentrations in water and soil samples along the Greens Bayou, (2) monitor the historical water quality data, and (3) identify and analyze land cover changes in the watershed using Landsat imagery. A total of 12 water and 12 soil samples, from four different sampling locations along the Greens Bayou, were collected during two seasons and processed for chemical analysis. Our water sample analysis revealed that the As, Cd, Pb, and Hg concentrations were higher in the fall compared with the summer and exceeded the critical limit. The soil analysis indicated that the Zn and Pb concentrations were higher in the fall over summer season and exceeded the background concentrations. Remote sensing analysis revealed that the impervious surface in the GBW increased by about 62.2% while the vegetative surface decreased by 30.6% during the period of 1984 to 2018. Environmental chemical analysis coupled with geospatial data demonstrated the impact of land cover changes on water and soil quality along the Greens Bayou by identifying areas vulnerable to change, which can be better managed to preserve the health of this urban watershed ecosystem.

Keywords Greens Bayou · Heavy metal · Remote sensing · Landsat and geographic information systems (GIS)

1 Introduction

Streams and bayous in urban watersheds are increasingly subjected to degradation by high inflow of nutrient, metal, and bacterial contaminants due to rapid land use and land cover changes. With 55% of world population living in urban areas and projected for increase to 68% by 2050, the impact on water and soil contamination is of immense importance to environmental and human health (UNDESA 2018). Houston, located in southeast of Texas, is the fourth largest city in the USA with a vast network of bayous that provide natural drainage to the sprawling urban area stretching over 600 square miles (Bogust 2017; Dart 2017). The southeast Texas region receives an average annual precipitation of 49.7 inches and has a flat landscape with an average elevation of 50 m above sea level, which contributes to the

B. B. M. Sridhar (✉)
Department of Earth and Environment, Florida International University, Miami, FL 33199, USA
e-mail: mbalajib@fiu.edu

J. Johnson
Department of Chemistry, Texas Southern University, Houston, TX 77004, USA

A. Mosuro
Department of Environmental and Interdisciplinary Sciences, Texas Southern University, Houston, TX 77004, USA

Published online: 30 September 2020

slow-moving drainage system. With Hurricane Harvey dumping 60.58 inches of rain in 2017 and tropical storm Imelda dropping 43.39 inches of rainfall in 2019, the flooding in the region is becoming more frequent in recent years (Freedman and Samenow 2019; Schaper 2017).

Increased land use and land cover changes in Houston-Galveston region of East Texas resulted in rapid expansion of impervious surfaces such as highways, roads, parking lots, drive ways, foot paths, roof tops, storm, and waste water drainage networks, altering significantly the natural biogeochemical cycle, hydrological flow pattern, and soil quality, and thus contributing to increased nutrient and metal runoff into urban waterways. The high runoff coefficient of the impervious surfaces compared with vegetative surfaces increase the pollutant loads into the urban streams and bayous (Carey et al. 2013). The impervious surface cover in the USA is projected to increase from 8 to 11 million hectares by 35% during the period of 2000 to 2030 (Theobald et al. 2009). An increase in impervious surface of over 20% is known to cause significant degradation of aquatic health (Exum et al. 2005).

Houston is one of the largest coastal cities in the USA, ranked as the fourth most populous city behind New York, Los Angeles, and Chicago (City of Houston 2018). Consequently, Houston has undergone rapid urbanization to sustain its growing population resulting in threat to the environmental and ecological health. Increase in impervious surface such as roads, parking lots, and sidewalks, and decrease in the vegetation, wetlands, and open surface areas are threatening the ecosystem of the Houston-Galveston region. Several point sources of pollution such as waste water outfalls, industrial outlets, and waste water treatment plants are distributed throughout the watersheds. Also, various non-point source pollutants from agricultural fields, household lawns, pet waste, automobiles, and construction sites enter into the surface waters of bayou due to runoff. The excess nutrient in runoff waters results in algal bloom increase, leading to the death of various fish (Thronson and Quigg 2008) and other aquatic species in the ecosystem, depending on the toxicity of the algal blooms (Dodds et al. 2009; Diaz and Rosenberg 2008).

Urban areas consist of both geochemical and anthropogenic sources of chemical contamination. Limestone, gypsum, gravel, and salt from weathering of rocks and soils make up the geologic sources of contamination which is specific to the geographical region. Apart from the industrial and domestic sewage effluents, anthropogenic sources of contamination also include several breakdown products from aging urban infrastructure such as concrete, asphalt, pipes, wiring, and roofing materials. The specific anthropogenic sources of metal contamination include Pb and Mn from vehicle emissions, Cu from brake emissions, Zn and Cd from vehicle tires, Cd from batteries, and Cr and Ni from metal plating (Rauch and Pacyna 2009; Yesilonis et al. 2008; Chambers et al. 2016). High fertilizer application to urban lawns, pet waste, and septic pipe leakage contributes to elevated N and P concentrations in bayous and streams. Higher Ca, K, Si, and S concentrations in urban areas can be sourced to break down products of concrete, gypsum, and other construction activities (Ai et al. 2015). The water quality of urban streams and bayou are strongly influenced by the anthropogenic and natural processes within the watershed (Pratt and Chang 2012).

Greens Bayou is 45 miles long, with an upper reach that flows in an eastward direction as well as a lower reach that flows southward into the Houston Ship Channel (HCFD 2011). The entire Greens Bayou flows within the Harris County in Texas. Greens Bayou has undergone various structural changes throughout the years. During the heavy rain events, as the waste water treatment plants cannot handle large amount of sewage and storm water inflow, the untreated water will be released into the bayou. Urban growth, population dynamics, and industrial expansion have significant impact on the decline of the Greens Bayou water quality. Hence, it is important to monitor and study the long-term land cover and water quality changes of Greens Bayou. In this research, the soil and water samples were collected and analyzed systematically using the traditional laboratory techniques and further correlated with the landscape changes using the remote sensing analysis and the historical flow and chemical data of the bayou. The goal of this study is to analyze the spatial and temporal, water and soil quality changes of the Greens Bayou. Specific objectives of the study were to (1) analyze the nutrient and heavy metal concentrations in water and soil samples along the Greens Bayou, (2) monitor the historical water quality data, and (3) identify and analyze land cover changes in the watershed using Landsat imagery.

2 Material and Methods

2.1 Historical Water Quality Data Analysis

To evaluate and monitor the changes in the physical and chemical characteristics over time in Greens Bayou, a historical water quality data analysis was conducted by downloading and processing the data from the United States Geological Survey (USGS) water quality database. The water quality data going as far back as 1967 was downloaded and processed from the lone USGS sampling site (29° 55′ 05″, 95° 18′ 24″) on the bayou to analyze the chemical concentration trends overtime. Specific physical, nutrient, metal, and bacterial parameters were analyzed to characterize the water quality of Greens Bayou. The nutrient concentrations of total N and P concentrations were analyzed to monitor the contamination of the bayou over time.

2.2 Sampling Locations along Greens Bayou

Water and soil sampling locations distributed across the Greens Bayou are shown in Fig. 1. A total of 12 water samples and 12 soil samples were collected from 4 different sampling locations along the bayou during the summer (pre-Hurricane Harvey period) and the fall season (post-Harvey period) of 2017. The water samples were collected in triplicates using a telescopic dipper into sterilized bottles and the soil samples in triplicates were collected using a core sampler and divided into 0–10 cm, 10–20 cm, and 20–30 cm depths. Only the results of surface soil (0–10 cm) analysis is presented in this paper. About three water and soil samples were collected from each of the sampling locations (Fig. 1) with a distance of at least 10 m apart between them and all the soil samples were collected at least 3 m away from the bank of the bayou. The samples G58.4, G50, and G49.4 were collected in the Upper Greens Bayou Watershed (UGBW) and G6.1 was collected from the Lower Greens Bayou Watershed (LGBW). The sample locations were named with a letter followed by a number as suffix where the letter stands for the name of the bayou and the number represents the distance of the sample site in kilometers from the mouth of the Greens Bayou. For example, G58.4 represents the sample site located at 58.4 km from mouth of the bayou. The sample locations were recorded using a handheld Global Positioning System (GPS) receiver. Samples were stored, transported immediately to the laboratory, and kept at − 4 °C until further chemical analysis was performed.

2.3 Chemical Analysis

Water samples collected were microwave acid digested using a microwave digestion unit using EPA 3015A method (Mars 6, CEM, Matthews, NC). About 45 ml of water sample was mixed with 5 ml of HNO_3 for acid digestion in the sealed microwave vessels. The vessel contents were cooled and filtered using Whatman 1 filter paper for further analysis. Soil samples were sieved, air-dried, and prepared for chemical analysis, where about 0.5 g of soil sample from each replicate was measured and microwave acid digested in 10 ml of HNO_3 using EPA 3050B (USEPA 1996) digestion method for soil. Finally, the samples were analyzed for Al, As, B, Ba, Ca, Cd, Co, Cu, Cr, Fe, K, Mg, Mn, Mo, Na, P, Pb, S, Sr, and Zn concentrations by using inductively coupled plasma mass spectrometry (ICP-MS, Agilent 7500 Series, Santa Clara, CA). Also, the total C and N concentrations of the samples were analyzed using the TCN Analyzer. Results of water and soil samples were statistically analyzed using the MINITAB statistical software (MINITAB Inc., State College, PA, USA).

An assessment index to measure the environmental concentrations of soil and water known as single element pollution index (SEPI) was applied (Pendias and Pendias 2001; Kloke 1979). The SEPI was calculated using the formula:

$$\mathrm{SEPI} = \frac{\text{Metal content in soil or water media}}{\text{Permissible level of metal in the media}}$$

The Texas Human Health (THH) protection and Texas Commission on Environmental Quality (TCEQ) background criteria were adapted as permissible level for water and soil concentrations, respectively (TCEQ 1999, 2014). The SEPI values of less than or equal to 1 was classified as low contamination, 1–3 as moderate contamination, and more than 3 was considered as high contamination (Chen et al. 2005; Al Obaidy and Al Mashhadi 2013). A combined pollution index (CPI) was calculated, to identify the effect of multi-element contamination, where CPI was calculated using the formula

$$\mathrm{CPI} = \frac{(\text{Metal content in media}/\text{Permissible level of metal in the media})}{\text{Number of metals}}$$

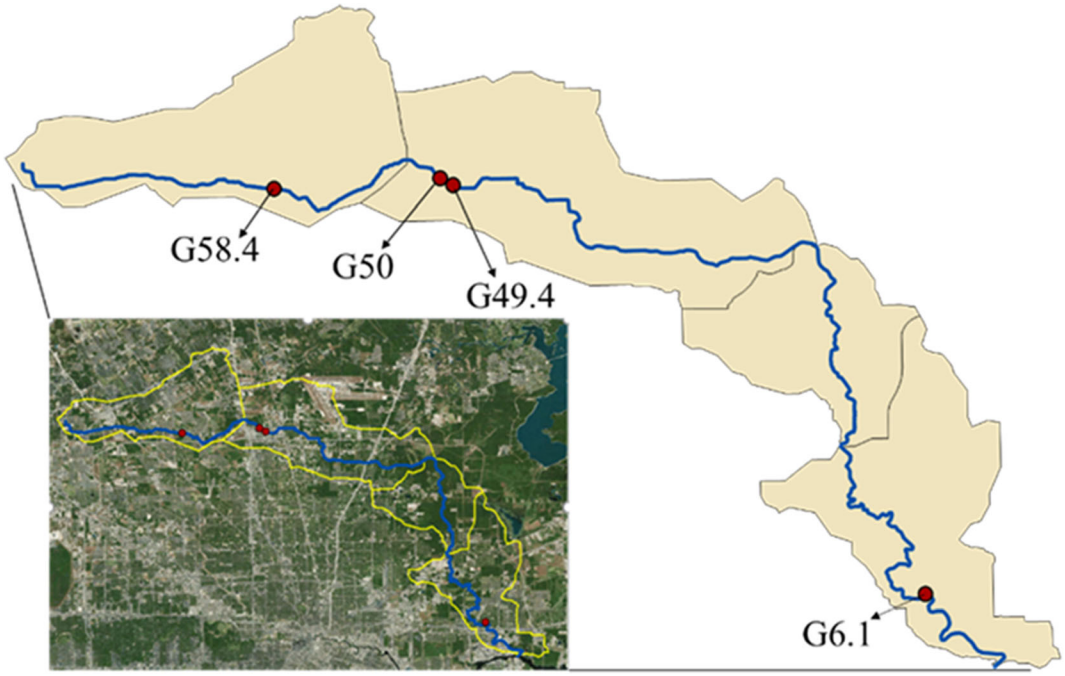

Fig. 1 The Greens Bayou watershed along with the sampling locations. The sampling locations named as G58.4, G50, G49.4 (Upper Greens Bayou Watershed), and G6.1 (Lower Greens Bayou Watershed) represent that they are 58.4, 50, 49.4, and 6.1 km from the mouth of the Greens Bayou. The subset image represents the overlay of Greens Bayou watershed on the natural color aerial imagery

The CPI values of less than or equal to 1 was classified as low contamination, 1–2 as moderate contamination, and more than 2 was considered as high contamination (Al Obaidy and Al Mashhadi 2013).

2.4 Statistical Analysis

The results of soil and water samples were statistically analyzed. The significant differences between the treatments were evaluated through the analysis of variance (ANOVA). Tukey's multiple range test was performed using MINITAB statistical analysis software (MINITAB Inc., State College, PA).

2.5 GIS Analysis

The flow lines, watershed boundary, and the flood hazard layers were extracted from the National Flood Hazard Layer (NFHL) database (https://www.floodmaps.fema.gov/NFHL/status.shtml) and Houston-Galveston Area Council GIS datasets (http://www.h-gac.com/gis-applications-and-data/datasets.aspx). Water and soil sampling points of the study area were imported into GIS as separate vector layer. The data were downloaded and processed using the Arc GIS Version 10.5 software (ESRI 2014).

2.6 Satellite Data Analysis

Five Landsat imagery from the time periods of (1) Aug 17, 1984, (2) Sept 16, 1989, (3) Aug 27, 1999, (4) Aug 22, 2009, and (5) Aug 26, 2018, all having 0% cloud cover, were chosen for this study. Landsat imagery were downloaded from USGS Earth Explorer (https://earthexplorer.usgs.gov/) website, and processed using the ER Mapper V16.6 software (Hexagon Geospatial 2020). Several single band and spectral ratio combinations were derived from the Dark Object Subtracted (DOS) values from each of the 7 bands in case of Landsat 5 imagery and from each of the 11 bands in case of Landsat 8 imagery. A DOS value of a spectral band is defined as one value less than the minimum digital number found in all pixels of that particular image for that spectral band (Vincent et al. 2004; Sridhar et al. 2009, 2011).

The vector data layers of GBW study area were overlaid and clipped, and the extracted study area from each of the Landsat imagery was then used for

subsequent analysis. The land cover changes were evaluated by mapping the vegetative and impervious surface characteristics as environmental indicators to map and monitor the landscape changes in GBW. Normalized difference vegetation index (NDVI) was calculated by using Eq. 1 (Rouse et al. 1974) for Landsat 5 imagery and using Eq. 2 for Landsat 8 imagery, to map the green vegetation in the study area. In Water Index (WI), Eq. 3 in the case of Landsat 5 imagery and Eq. 4 in the case of Landsat 8 imagery were used to map the water content in the study area (Sridhar and Gidudu 2020). An impervious surface area index (ISAI), Eq. 5 was used to map the impervious surface areas in the Landsat 5 imagery while Eq. 6 was used for the Landsat 8 imagery (Sridhar and Gidudu 2020). The spatial and temporal changes in impervious, water, and vegetative surface areas from 1995 to 2019 were mapped, classified, and quantified individually for each of the selected images of GBW. Finally, the chemical analysis data and spatial and temporal data were integrated to analyze the overall landscape change pattern, in GBW.

$$\mathrm{NDVI} = \frac{\mathrm{Band\ 4} - \mathrm{Band\ 3}}{\mathrm{Band\ 4} + \mathrm{Band\ 3}} \quad (1)$$

$$\mathrm{NDVI} = \frac{\mathrm{Band\ 5} - \mathrm{Band\ 4}}{\mathrm{Band\ 5} + \mathrm{Band\ 4}} \quad (2)$$

$$\mathrm{WI} = \frac{\mathrm{Band\ 2}}{\mathrm{Band\ 5}} \quad (3)$$

$$\mathrm{WI} = \frac{\mathrm{Band\ 1}}{\mathrm{Band\ 6}} \quad (4)$$

$$\mathrm{ISAI} = \sqrt{\mathrm{Band\ 6\ x\ Band\ 3}} \quad (5)$$

$$\mathrm{ISAI} = \sqrt{\mathrm{Band\ 10\ x\ Band\ 3}} \quad (6)$$

Landsat image classification accuracy assessment was conducted with reference of 187 random ground-truth sampling points that were collected with GPS device in the field and using high-resolution Google earth imagery for assessment of every classified image. The data is summarized and quantified by using error matrices.

3 Results

Our historical data analysis shows that the total N and P concentrations in Greens Bayou were collected only at one sampling location from the 1970s to the 2000s and the N and P were not analyzed in the samples there after. The total N concentrations (Fig. 2a) did show neither a decreasing nor an increasing trend while the P concentrations (Fig. 2b) showed a decreasing trend with time. The intensity of the sampling was more in the early than the later periods. The N (Fig. 2c) and P (Fig. 2d) concentration of water was high during low water discharge in the bayou and the concentration decreased rapidly at peak water flow in the bayou. The historical sampling site was located downstream to the G49.4 sampling location and no active sampling was conducted in this study due to lack of access.

The concentrations of total carbon (C), N, P, K, Ca, Mg, S, and Na of the water samples are given in Table 1. Our results show that the C, N, P, K, Mg, and Na concentrations in the upstream (G58.4, G50, and G49.4) of Greens Bayou were significantly higher than the downstream (G6.1) in the summer (Table 1). Conversely, the concentrations of K, Ca, Mg, S, and Na in the G6.1 were significantly higher than the upstream locations of the bayou in fall (Table 1). The N concentrations in G58.4 in summer and G58.4, G50, and G49.4 in fall exceeded the Texas Human Health (THH) criteria of 10 ppm concentration in water samples. The P concentrations in all the sampling locations were well above the recommended maximum level of 0.1 ppm which is the proposed critical limit of EPA for algal bloom occurrence in surface water (Table 1). The Cu, Zn, Cr, Co, and Ni concentrations in water samples collected during both seasons remain low with no difference between the upstream and downstream locations (Table 2). The As concentration in G58.4 during summer and G49.4 during fall season remain above the THH and EPA criteria of 10 ppb. The Cd concentration in the G50 and G49.4 during fall remains above the THH and EPA criteria of 5 ppb (TCEQ 2014; USEPA 2018). The Pb concentration in all the sampling locations remains above the THH criteria of 1.15 ppb (Table 2). The Pb concentrations in fall were higher compared with summer. The Hg concentrations in all the sampling locations during both seasons remain above the THH criteria of 0.01 ppb (Table 2).

The concentrations of C, N, P, K, Ca, Mg, and S in soil samples do not show any significant spatial and

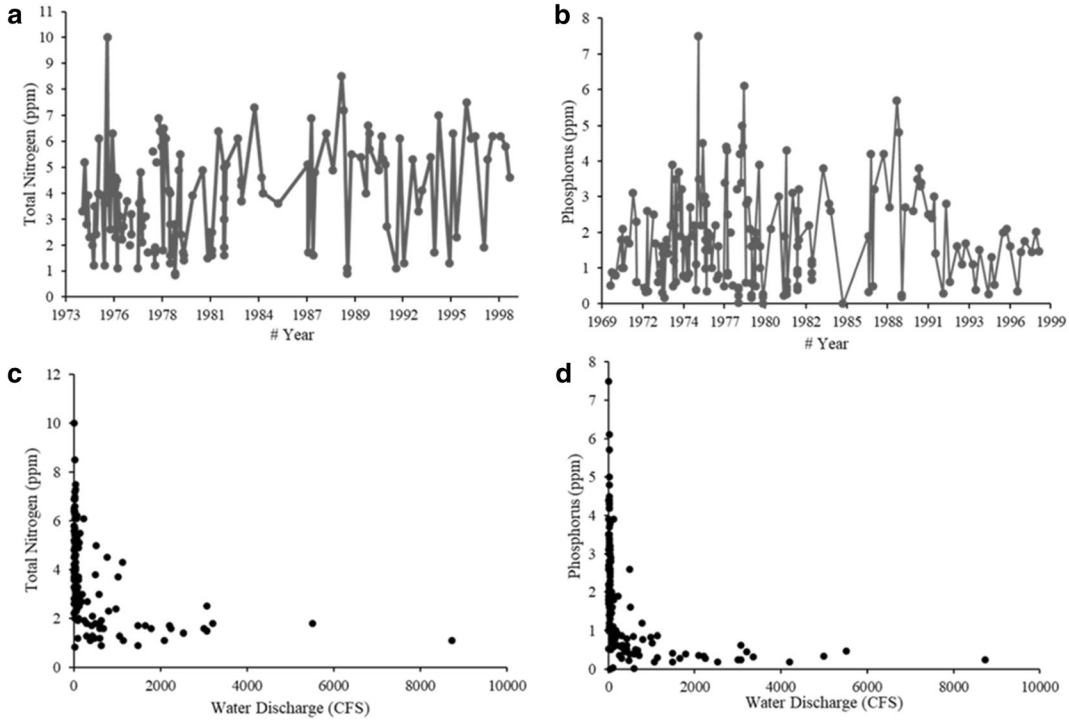

Fig. 2 Historical concentrations of the total nitrogen (**a**) and phosphorus (**b**) in the water samples of the Greens Bayou. Nitrogen and phosphorus concentrations decreased with increase in the flow of the bayou. The bayou water data was available for the during the period of 1969–1999 intermittently

temporal differences (Table 3). The Na and S in fall and K concentrations in summer remained higher at G50 compared with other locations (Table 3). The Cu, As, Cr, and Cd soil concentrations remain below the soil background concentrations during both seasons. No significant spatial and temporal differences were found between the sampling locations. The Zn soil concentrations in all the sampling locations during both seasons remain above the soil background levels of 30 ppm (Table 4). The Pb concentration in the G58.4 during fall remains above the soil background level of 15 ppm (Table 4).

The SEPI value of water samples for As, Cd, Pb, and Hg was higher in fall compared with summer (Table 5). The As and Cd values were higher in downstream during fall season and is classified as moderately contaminated, as their SEPI values fall between the range of 1–3. The water samples all along the bayou were moderately contaminated with SEPI values of Pb in the range of 1–3 in summer and turned to higher contamination with values exceeding the value of 3 in fall. The Hg contamination is classified high as the SEPI values exceeded 3 during both the sampling seasons. The CEPI values of the water indicate that the combined metal contamination value of the water is low during both seasons all along the bayou (Table 5). The SEPI value of Zn in the soil samples remains high in the summer compared with the fall season. All the soil samples along the bayou were moderately polluted with Zn. The Zn contamination remained high in the upstream at G58.4, G50, and G49.4 and decreased along the downstream at G6.1. The SEPI value of Pb ranged from 0.5 to 1.1 indicating lower soil contamination along the bayou during both seasons (Table 5). The CEPI values of soil ranged from 0.5 to 1 indicating lower level of contamination in the flood plain soils of GBW.

The pseudo color Landsat imagery of the Greens Bayou Watershed (GBW) where Landsat 5 bands 2, 3, and 4 were shown in blue, green, and red, respectively, and in the case of Landsat 8 imagery, bands 3, 4, and 5 were shown in blue, green, and red, respectively, showing that the urban impervious surface increased significantly from 1984 to 2018 at the expense of the vegetative cover (Fig. 3). The gradual progression of the urban sprawl all along the watershed can be seen distinctly. An unsupervised classification of the Landsat imagery with the ratio inputs of WI, NDVI, and ISAI showed that the GBW has significant increase in the impervious surface during the course of

Table 1 Nutrient and other major elemental concentration in water samples collected from Greens Bayou (in mg L^{-1}). Given are mean values ($n = 3$) of three replicates. Also given are the proposed critical limits for human health protection in water for specific metals (TCEQ 2014; USEPA 2018). *THH*, Texas Human Health protection criteria

Sampling locations	C	N	P	K	Ca	Mg	S	Na
Summer								
G58.4	32.5 a	*13.2* a	2.1 a	11.4 a	55.0	11.0 a	6.9	72.0 a
G50	36.4 a	9.0 a	1.9 a	10.3 ab	46.1	9.3 a	6.7	72.4 a
G49.4	32.9 a	7.6 b	2.2 a	12.4 a	50.6	9.2 a	7.9	82.6 a
G6.1	21.4 b	5.3 b	0.2 b	4.2 b	29.0	4.5 b	3.6	23.1 b
Fall								
G58.4	30.2 c	*14.0* a	1.9 a	8.7 b	44.8 ab	7.8 b	7.9 b	59.4 b
G50	33.5 a	*12.8* b	2.2 a	9.1 b	41.3 b	8.4 b	7.8 b	62.6 b
G49.4	31.6 b	*11.3* c	2.1 a	9.5 b	39.8 b	8.7 b	8.9 b	63.1 b
G6.1	31.5 b	9.4 d	1.3 b	17.8 a	53.4 a	37.6 a	23.3 a	*296.2* a
Criteria								
THH		10						
EPA								200

† Means followed by a different letter are significantly different at the 0.05 probability level, grouped into classes a, b, and c. The italicized values exceed the proposed critical limits

last three decades (Fig. 4). The impervious surface area in the watershed increased by 62.2% from 1984 to 2018 while the vegetative cover decreased by 30.6% over the same period (Fig. 5).

To identify the extent of land cover changes within the 500-year flood plain of the GBW, vector outline of the 500-year flood plain of Greens Bayou was downloaded, overlaid on the GBW area, and analyzed. Impervious surface area has consistently increased and the vegetative surface area decreased within the GBW flood plain area from 1984 to 2018 (Fig. 6). The loss of vegetation along the stream in northwestern and

Table 2 Heavy metal concentrations in the water samples collected from the different locations along the Greens Bayou (in μg L^{-1}). Given are mean values ($n = 3$) of three replicates. Also given are the proposed critical limits for human health protection in water for specific metals (TCEQ 2014; USEPA 2018). *THH*, Texas Human Health protection criteria

Sampling locations	Cu	Zn	As	Cr	Cd	Pb	Hg	Co	Ni
Summer									
G58.4	16.9	33.6	*10*	0.06	0.57	*7.21*	*0.05* a	0.91	3.17
G50	29.3	91.4	5.8	1.16	1.93	*2.88*	*0.02* b	1.17	3.34
G49.4	31.3	44.1	7.8	0.24	1.52	*2.71*	*0.04* a	1.03	2.25
G6.1	16.3	13.7	8.4	0.54	0.09	*1.47*	*0.06* a	0.55	0.65
Fall									
G58.4	57.7	65.1	6.3	1.08 b	1.04	*4.77*	*0.02* b	0.41	2.45
G50	48.9	130.4	8.9	0.65 b	*9.23*	*9.30*	*0.06* a	0.56	2.07
G49.4	47.5	95.5	*11.6*	0.90 b	*6.79*	*5.66*		0.60	2.15
G6.1	49.7	108.4	7.2	3.00 a	3.74	*7.34*		0.49	3.31
Criteria									
THH			10	62	5	1.15	0.012		
EPA	2		10	50	5	10	1		20

† Means followed by a different letter are significantly different at the 0.05 probability level, grouped into classes a, b, and c. The italicized values exceed the proposed critical limits

Table 3 Nutrient and other major elemental concentration in flood plain soil samples collected from Greens Bayou (in mg kg^{-1}). Given are mean values ($n = 3$) of three replicates

Sampling locations	C (%)	N	P	K	Ca	Mg	S	Na
Summer								
G58.4	3.3		298	301 ab	8272	2995	179	640
G50	4.2		285	498 a	10,778	2474	252	562
G49.4	0.4		218	283 b	11,394	2400	189	582
G6.1	0.01		264	269 b	12,530	2409	222	295
Fall								
G58.4	1.5	842	180	777	21,787	3069	123 b	403 b
G50	1.9	2334	245	522	14,529	2568	242 a	1101 a
G49.4	2.4	1265	167	593	17,750	2667	143 b	269 b
G6.1	1.4	289	123	361	11,986	2171	169 b	261 b

† Means followed by a different letter are significantly different at the 0.05 probability level, grouped into classes a, b, and c

southeastern areas of the GBW is significant. The impervious surface area in the 500-year flood plain of GBW increased by 15.3% from 1984 to 2018 while the vegetative cover decreased by 5.9% over the same period (Fig. 7). The relationship between the land cover changes and the water discharge in the Greens Bayou during the last three decades is shown in Fig. 8. The increase in the impervious surface and decrease in vegetative surface in the GBW resulted in increased surface runoff and flooding, contributing to the increase in water flow and discharge into the bayou over the course of time. The accuracy assessment of each classified Landsat image from 1984 to 2018 is given in Table 6. The overall accuracy of the imagery ranged from 89.4 to 96.9% and the kappa statistic ranged from 0.82 to 0.95 for the selected imagery (Table 6).

4 Discussion

The N and P concentration in the Greens bayou water ranging at 5.3 to 14.2 mg l^{-1} and 0.2 to 2.2 mg l^{-1}, respectively, during both seasons exceeded the typical US urban storm water concentration of 2.0 mg l^{-1} for N and 0.26 mg l^{-1} for P (Schueler 2003; Carey et al. 2013). Historically, the bayou is eutrophic with enriched N and

Table 4 Heavy metal concentrations in the soil samples collected from the different locations along the Greens Bayou (in mg kg^{-1}). Given are mean values ($n = 3$) of three replicates. Also given are the proposed Texas-specific soil background concentrations (TCEQ 1999)

Sampling locations	Cu	Zn	As	Cr	Cd	Pb	Hg
Summer							
G58.4	12.5	82.8	2.8	21.0	0.15 b	10.7	0.004
G50	9.1	59.5	3.5	17.6	0.09 b	7.3	0.002
G49.4	8.7	51.8	2.2	16.5	0.14 b	8.2	0.003
G6.1	8.2	54.5	2.0	19.9	0.42 a	10.7	0.007
Fall							
G58.4	8.5	52 a	2.2 a	20.4	0.7	17.0	0.00
G50	10.0	69 a	0.6 b	19.8	0.4	11.5	0.01
G49.4	6.1	42 b	0.6 b	19.2	0.6	12.2	0.01
G6.1	4.5	38 b	1.3 b	24.1	0.4	11.0	0.01
Criteria							
Background	15	30	5.9	30		15	0.04

† Means followed by a different letter are significantly different at the 0.05 probability level, grouped into classes a, b, and c

Table 5 Single element pollution index (SEPI) and combined pollution index (CPI) of water and soil samples collected from the different locations along the Greens Bayou (in mg kg^{-1}). Given are mean values ($n = 3$) of three replicates

Sampling locations	As	Cd	Pb	Hg	CPI	Zn	Pb	CPI
	Water samples					Soil samples		
Summer								
G58.4	1.0	0.1	6.3	4.2	0.2	2.8	0.7	1.0
G50	0.6	0.4	2.5	1.7	0.1	2.0	0.5	0.7
G49.4	0.8	0.3	2.4	3.3	0.1	1.7	0.5	0.7
G6.1	0.8		1.3	5.0	0.1	1.8	0.7	0.7
Fall								
G58.4	0.6	0.2	4.1	1.7	0.1	1.7	1.1	0.8
G50	0.9	1.8	8.1	5.0	0.2	2.3	0.8	0.9
G49.4	1.2	1.4	4.9		0.1	1.4	0.8	0.6
G6.1	0.7	0.7	6.4		0.1	1.3	0.7	0.5

P concentrations reaching up to 10 and 7.5 ppm, respectively (Fig. 2). The P concentration in the range of 10 to 75 ppb is the appropriate level to control the nuisance algal blooms in fresh water (USEPA 2002). High N, P, and other nutrient concentrations in the bayou water (Table 1) can be attributed to the domestic and

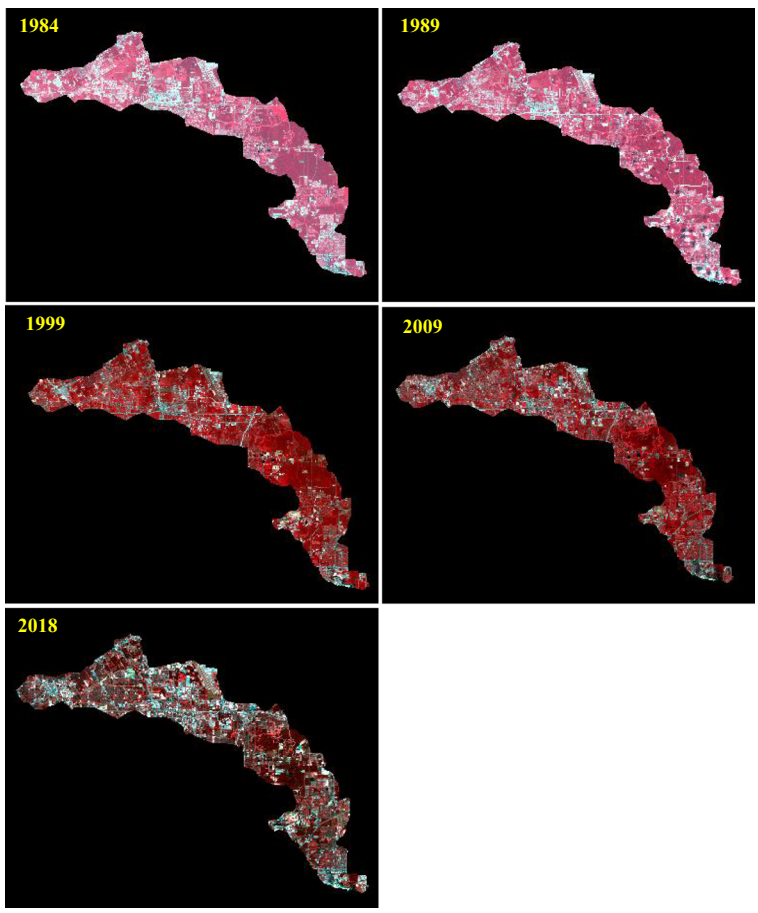

Fig. 3 The pseudo color image of the Greens Bayou watershed where Landsat 5 bands 2, 3, and 4 were shown in blue, green, and red, respectively, while the Landsat 8 bands 3, 4, and 5 were shown in blue, green, and red, respectively. The vegetation appears in shades of red while the urban areas appear in pale white to lighter shades, and the wetland areas and water appear dark. The western part of the study area is dominated by urban impervious surface while the eastern part by vegetation

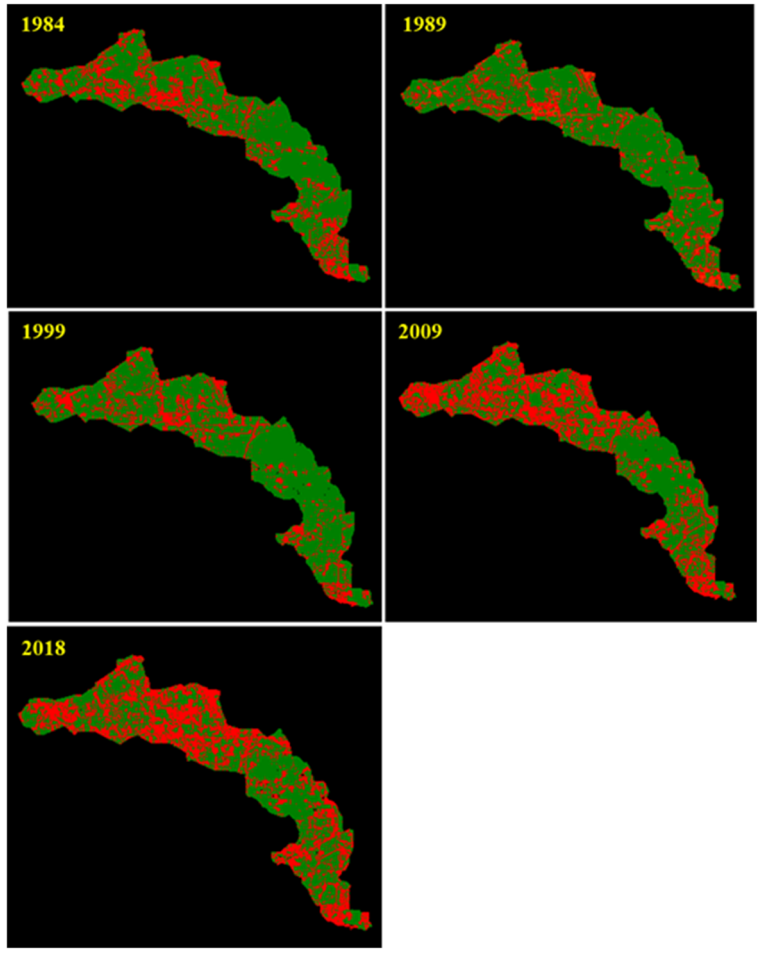

Fig. 4 The unsupervised classification images of the study area where the areas covered with vegetative surface, impervious surface, and water are shown in green, red, and blue, respectively. The impervious surface areas increased at the expense of the vegetative cover during the period of 1995–2019

municipal wastewater disposal as well as intensification of runoff from residential yards, roads, agricultural, and industrial activities within the watershed. The discharge from wastewater treatment plants (WWTP) is a major factor affecting the nutrient loads in urban streams (Andersen et al. 2004; Ekka et al. 2006; Carey et al. 2013). The high concentration of Na in G6.1 in fall, which is above the EPA criteria limit of 200 ppm, can be attributed to the Hurricane Harvey which resulted in slow drainage and backing up of estuary into the bayou.

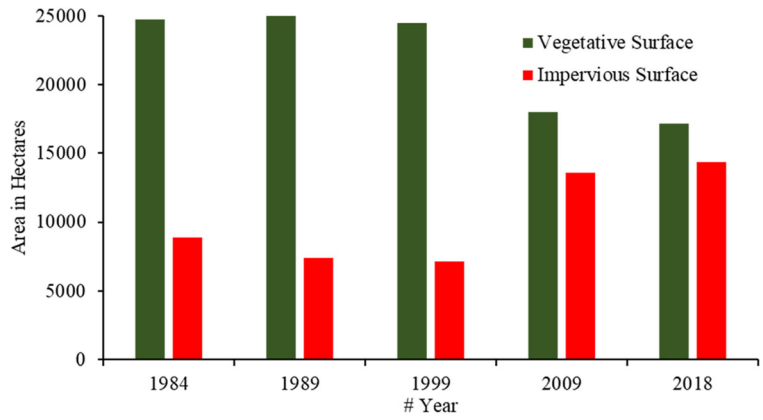

Fig. 5 Change in the area of impervious and vegetative surface over the period of 1984–2018 in the Greens Bayou Watershed (GBW)

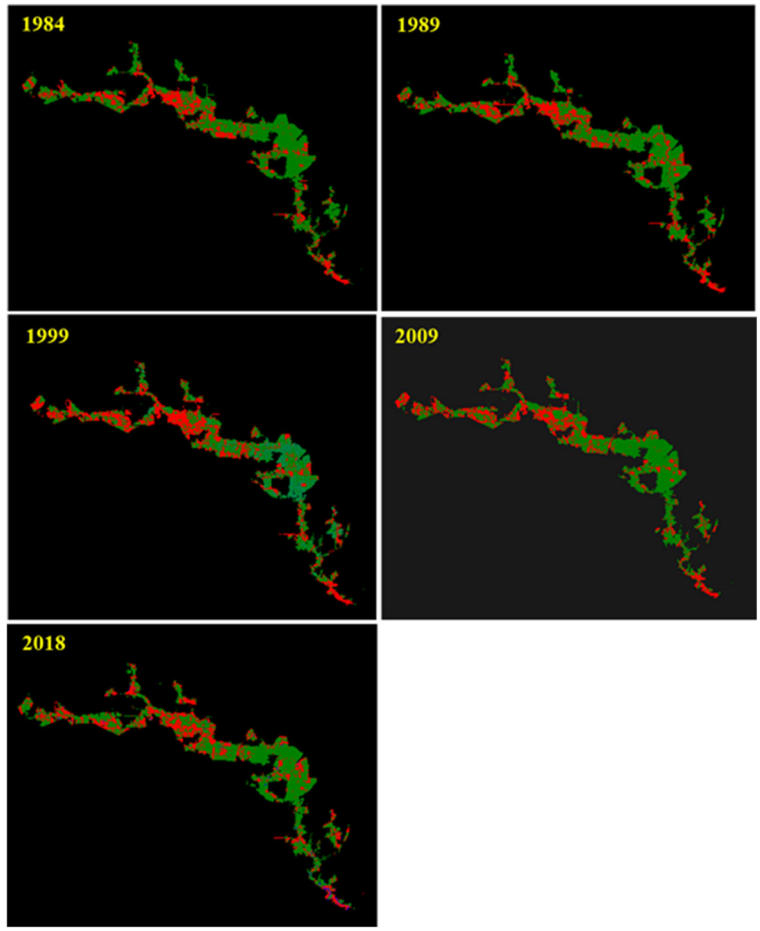

Fig. 6 The unsupervised classification images of the 500-year flood plain of Greens Bayou Watershed (GBW) where the areas covered with vegetative surface, impervious surface, and water are shown in green, red, and blue, respectively. The impervious surface areas increased at the expense of the vegetative cover during the period of 1984–2018

The decrease in P concentration with time in the historical water samples (Fig. 2b) can be attributed to the emergence of low P laundry detergents and cleaning compounds in the 1990s (Litke 1999) and application of lime amendments to limit P availability in WWTP effluents (Meeroff et al. 2008). Contribution of atmospheric deposition of N (Smil 2000; Carey et al. 2013) along with surface runoff may be the reason for higher concentrations of N over P with time in the historical water samples (Fig. 2a).

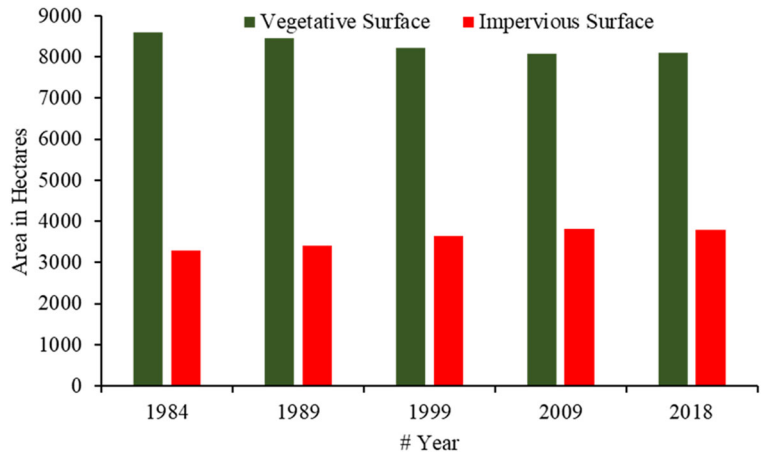

Fig. 7 Change in the acerage of impervious and vegetative surface within the 500-year flood plain of Greens Bayou Watershed (GBW) over the period of 1984–2018

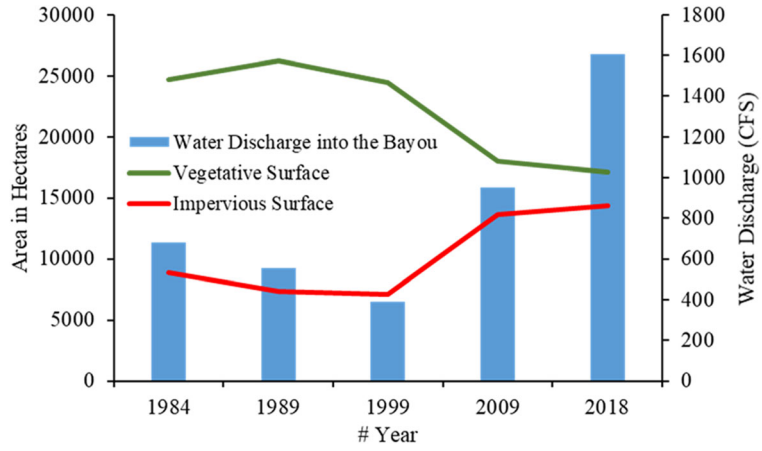

Fig. 8 Land cover changes in the Greens Bayou Watershed (GBW) and the water discharge in the Greens bayou during the period of 1984–2018

The concentration of As (Table 2) is significantly higher all along the bayou and is also higher than the general range of As in natural water which is 1–2 ppb (Hindmarsh and McCurdy 1986; USNRC 1999; WHO 2011a). Exposure to high As concentration in water increases the risk of cancer to the skin, lung, bladder, and kidney (IPCS 2001). The concentration of Pb is higher than the THH criteria of 1.15 ppb and getting close to the EPA proposed maximum critical limit of 10 ppb (Table 2). High concentration of Pb in water is poisonous affecting the health of infants and children (WHO 2011b). The high concentration of As, Pb, and Cd in fall over the summer can be attributed to the Hurricane Harvey flooding during which the industrial and WWTP released high volume of untreated effluents into the bayous. High metal and nutrient concentration in Greens Bayou can be attributed to the presence of several WWTP outfalls, large- and small-scale industries, and high impervious surface area within the drainage watershed. WWTP and storm water runoff are considered as large sources of surface water pollution in urban areas (Paul and Meyer 2001; Roberto et al. 2018). The soil nutrient and metal concentrations remain similar among the sites with less seasonal variation except for the Cr and Pb which remained higher in the fall compared with summer (Tables 3 and 4).

The overall Landsat classification accuracy is 95.3%, 89.4%, 92.1%, 93.7%, and 96.9%, respectively, for the imagery of 1984 to 2018 (Table 6), which is higher than the suggested minimum level of interpretation accuracy of 85% (Anderson et al. 1976). The user's and producer's accuracy for the vegetative and impervious surface cover land cover was found to be high (Table 6), which is sufficient to produce an overview of the landscape change pattern within the watershed. The land cover category of water had low producer's accuracy, which means that some of the ground reference points of this category were classified incorrectly (Table 6). The reason being the bayou flow drops down significantly during the periods of low precipitation and runoff. The low overall classification accuracy of 89.4% and kappa statistic of 0.82 was found in the case of the 1989 image because of the slight cloud cover found in the southernmost part of the watershed (Table 6; Fig. 3). The highest classification

Table 6 Summary of user's, producer's, overall accuracy (%), and kappa statistic of land cover change maps

Land cover	1984		1989		1999		2009		2018	
	User.	Prod.	User.	Prod.	User.	Prod.	User.	Prod.	User.	Prod.
Vegetative surface	98.9	100	86	98.9	92.5	98.9	94.6	100	94.6	100
Impervious surface	90.1	100	91.3	86.3	90.5	91.8	90.8	94.5	98.6	94.5
Water	100	69	100	69.1	92.5	72.4	100	72.4	100	93.1
Overall accuracy	95.3		89.4		92.1		93.7		96.9	
Kappa statistic	0.92		0.82		0.87		0.90		0.95	

accuracy of 96.9% and kappa statistic of 0.82 was found in 2018 image, which is a Landsat 8 image with high radiometric and spectral resolution compared with all other images which were of Landsat 5.

The land cover change analysis revealed that the impervious surface increased by 62.2% and the vegetative surface decreased by 30.6% in the GBW during the period of last three decades (Figs. 4 and 5). The total impervious surface percentage, which is the ratio percentage of total impervious surface to the total area of the GBW, increased from 20.6% in 1984 to 42.8% in 2018. A 5–10% increase in total impervious surface (Schiff and Benoit 2007) in a watershed can impair water quality while 10–20% (Exum et al. 2005) will cause significant aquatic degradation (Carey et al. 2013). The land cover analysis within the 500-year flood plain of GBW revealed a 15.3% increase in impervious surface and 5.9% decrease in vegetative surface within GBW during the period of last three decades (Figs. 6 and 7). The total impervious surface percentage within the 500-year flood plain of GBW increased from 23.6% in 1984 to 27.2% in 2018.

The 500-year floods are getting more frequent in Houston-Galveston region with several watersheds experiencing the large flood events, at least 4–5 times within the last decade. Houston experienced three 500-year storms back to back in 2015, 2016, and 2018, respectively. During Hurricane Harvey in 2018, about 153,000 homes that got flooded were located outside the 100-year flood plain (Despart 2018) and 84% of the structures within the 500-year flood plain got flooded (Cardenas and Formby 2018). Hence, Houston regional flood plain maps were considered outdated and inaccurate and Harris county started the process of redrawing the maps (Despart 2018). Therefore, we chose to evaluate the land cover changes within the 500-year flood plain of GBW instead of 100-year flood plain. The vegetative surface area within 500-year flood plain of GBW should be increased to improve bayou water quality and to reduce flood impacts.

5 Conclusions

Land cover change due to human activities is an important parameter that impacts the global environmental and ecological change by changing complex biophysical processes at global, regional, and local scales (Wasige et al. 2013; Wu et al. 2003). Impervious surface increase in GBW and within 500-year flood plain of GBW effectively alters hydrological pathways and enhances nutrient transport, and thus impacts the natural biogeochemical cycle of the region. High concentration of N, P, Na, Cu, Zn, As, Cr, and Pb in fall over summer water samples can be attributed to Hurricane Harvey flooding which overwhelmed the waste water treatment and industrial plants along the bayou. The Zn and Pb concentration built up in soils is evident as their metal concentrations exceeded the background soil concentrations. Similarly, the concentrations of As, Cd, and Pb in water exceeded the safety limits for human health. The nutrient and metal increase in water and soils of GBW can be attributed to several point and non-point pollutant source locations in the downstream, as several waste water outlets dump all along the length of the Greens bayou. The total N and P concentrations in our water samples as well as the historical data exceeds the EPA nutrient criteria for rivers and streams which is 0.76 ppm for total N and 0.128 ppm for total P, exceeding which results in eutrophication of water bodies. The seasonal variation is more prominent in the water samples compared with soil samples. The natural low flow period in summer resulted in high nutrient and metal concentrations in the upstream while the high discharge in fall resulted in the high downstream concentrations. Continuous in situ sensors of water quality parameters will promote the better understanding of the urban bayou systems.

The increasing impervious surface over the low and decreasing vegetative surface in both the watershed and the 500-year flood plain increases the velocity and volume of surface water runoff. Optimizing watershed management practices to reduce chemical inflow and decrease the flood water runoff is critical to improve the water and soil quality of GBW. This study improves the understanding of the land cover change in GBW which is recognized as a critical gap in the knowledge of vegetation loss, soil and water degradation, and eutrophication of Galveston Bay. Further research involving the use of high-resolution satellite and aerial imagery along with a comprehensive water analysis for extensive inorganic and organic contaminants covering the entire watershed will be greatly beneficial. Urban growth with environmental sustainability is key to the future economic growth in the region where urban development should be planned by conserving the natural resources. Conservation of the wetland areas, reducing the inflow of domestic sewage and

industrial effluents, developing and preserving the vegetative buffer strips around the drainage streams, along with the control of point and non-point source pollution, is crucial to prevent the decline in the water quality and to promote urban watershed sustainability.

Acknowledgments We acknowledge Ms. Djene Keita for the chemical analysis of water and soil samples and Mr. Adesope, Mr. Habibur, and Ms. Malikiya for help in water and soil sampling.

Funding This research was primarily supported by the National Science Foundation (NSF) through the Texas Southern University (TSU) under the award numbers HRD-1622993 and BCS-1831205.

References

Ai, L., Shi, Z. H., Yin, W., & Huang, X. (2015). Spatial and seasonal patterns in stream water contamination across mountainous watersheds: Linkage with landscape characteristics. *Journal of Hydrology, 523*, 398–408.

Al Obaidy, A. H. M. J., & Al Mashhadi, A. A. M. (2013). Heavy metal contaminations in urban soil within Baghdad city, Iraq. *Journal of Environmental Protection, 4*, 72–82.

Andersen, C. B., Lewis, G. P., Sargent, K. A., & Sarkar, D. (2004). Influence of waste water treatment effluent on concentrations and fluxes of solutes in the Bush River, South Carolina, during extreme drought conditions. *Environmental Geosciences, 11*, 28–41.

Anderson, J.R., Hardy, E.E., Roach, J.T., & Witmer, R.E. (1976). A land use and land cover classification system for use with remote sensor data. Circular 761. Washington, DC, USA. https://pubs.er.usgs.gov/publication/pp964. Accessed 14 September 2020.

Bogust, I. (2017). *Houston's flood is a design problem*. The Atlantic. https://www.theatlantic.com/technology/archive/2017/08/why-cities-flood/538251/. Accessed 5 June 2020.

Cardenas, C., & Formby, B. (2018). Houston council approves changes to floodplain regulations in effort to reduce flood damage. https://www.texastribune.org/2018/04/04/houston-city-council-approves-changes-floodplain-regulations-narrow-vo/. Accessed 15 September 2020.

Carey, R. O., Hochmuth, G. J., Martinez, C. J., Boyer, T. H., Dukes, M. D., Toor, G. S., & Cisar, J. L. (2013). Evaluating nutrient impacts in urban watersheds: Challenges and research opportunities. *Environmental Pollution, 173*, 138–149.

Chambers, L. G., Chin, Y., Filippelli, G. M., Gardner, C. B., Herndon, E. M., Long, D. T., Lyons, W. B., Macpherson, G. L., McElmurry, S. P., McLean, C. E., Moore, J., Moyer, R. P., Neumann, K., Nezat, C. A., Soderberg, K., Teutsch, N., & Widom, E. (2016). Developing the scientific framework for urban geochemistry. *Applied Geochemistry, 67*, 1–20.

Chen, T. B., Zheng, Y. M., Lei, M., Huang, Z. C., Wu, H. T., Chen, H., Fan, K. K., Yu, K., Wu, X., & Tian, Q. Z. (2005). Assessment of heavy metal pollution in surface soils of urban parks in Beijing, China. *Chemosphere, 60*(4), 542–551.

City of Houston. (2018). Facts and figures. http://www.houstontx.gov/abouthouston/houstonfacts.html. Accessed 5 June 2020.

Dart, T. (2017). The bayou's alive: Ignoring it could kill Houston. The Guardian. https://www.theguardian.com/cities/2017/dec/20/bayou-houston-flood-hurricane-harvey-texas-resilience. Accessed 5 June 2020

Despart, Z. (2018). Harris county to begin work on new flood plain maps. https://www.chron.com/politics/houston/article/Harris-County-to-begin-work-on-new-floodplain-maps-13256550.php. Accessed 15 September 2020.

Diaz, R. J., & Rosenberg, R. (2008). Spreading dead zones and consequences for marine ecosystems. *Science, 321*, 926–929.

Dodds, W. K., Bouska, W. W., Eitzmann, J. L., Pilger, T. J., Pitts, K. L., Riley, A. J., Schloesser, J. T., & Thornbrugh, D. J. (2009). Eutrophication of U.S. freshwaters: Analysis of potential economic damages. *Environmental Science and Technology, 43*(1), 12–19.

Ekka, S. A., Haggard, B. E., Matlock, M. D., & Chaubey, I. (2006). Dissolved phosphorus concentrations and sediment interactions in effluent-dominated Ozark streams. *Ecological Engineering, 26*, 375–391.

ESRI. (2014). *Arc GIS Desktop-Environmental Systems Research Institute Software (Version 10.3)*. Available from https://desktop.arcgis.com/en/arcmap/10.5/get-started/main/get-started-with-arcmap.htm.

Exum, L. R., Bird, S. L., Harrison, J., & Perkins, C. A. (2005). *Estimating and projecting impervious cover in the Southeastern United States* (pp. 1–133). Washington, D.C: U.S. Environmental Protection Agency.

Freedman A., & Samenow, J. (2019). Flooded again: Climate change is making flooding more frequent in Southeast Texas. https://www.washingtonpost.com/weather/2019/09/20/flooded-again-climate-change-is-making-flooding-more-frequent-southeast-texasthanks-part-climate-change/. Accessed 5 June 2020.

HCFD. (2011) Green bayou watershed factsheet. https://www.hcfcd.org/media/1291/greensbayou_factsheetrvsd.pdf. Accessed 5 June 2020.

Hexagon Geospatial. (2020). *ERDAS ER Mapper Software (Version- 16.6.0.630)*. Available from https://download.hexagongeospatial.com/en/downloads/imagine/erdas-er-mapper-2020.

Hindmarsh, J. T., & McCurdy, R. F. (1986). Clinical and environmental aspects of arsenic toxicity. *CRC Critical Reviews in Clinical Laboratory Sciences, 23*, 315–347.

IPCS. (2001). *Arsenic and arsenic compounds*. Geneva, World Health Organization, International Programme on Chemical Safety, Environmental Health Criteria (p. 224). https://www.who.int/ipcs/publications/ehc/ehc_224/en/. Accessed 1 February 2020.

Kloke, A. (1979). Content of arsenic, cadmium, chromium, fluorite, lead, mercury and nickel in plants grown on contaminated soil. Paper Presented at United Nations ECE Symposium, on Effects of Airborne Pollution on Vegetation, Warsaw.

Litke, D. W. (1999). *Review of phosphorus control measures in the United States and their effects on water quality*. U.S. Geological Survey: Denver.

Meeroff, D. E., Bloetscher, F., Bocca, T., & Morin, F. (2008). Evaluation of water quality impacts of on-site treatment and

disposal systems on urban coastal waters. *Water, Air, and Soil Pollution, 192*, 11–24.

Paul, M. J., & Meyer, J. L. (2001). Streams in the urban landscape. *Annual Review of Ecology and Systematics, 32*, 333–365.

Pendias, A. K., & Pendias, H. (2001). *Trace element in soils and plants*. London: CRC Press.

Pratt, B., & Chang, H. (2012). Effects of land cover, topography, and built structure on seasonal water quality at multiple spatial scales. *Journal of Hazardous Materials, 209–210*, 45–58.

Rauch, J. N., & Pacyna, J. M. (2009). Earth's global Ag, Al, Cr, Cu, Fe, Ni, Pb, and Zn cycles. *Global Biogeochemical Cycles, 23*, GB2001. https://doi.org/10.1029/2008GB003376.

Roberto, A. A., Gray, J. B. V., & Leff, L. G. (2018). Sediment bacteria in an urban stream: Spatiotemporal patterns in community composition. *Water Research, 134*, 353–369.

Rouse, J.W., Haas, R.H., Schelle, J.A., Deering, D.W., & Harlan, J.C. (1974). Monitoring the vernal advancement and retrogradation (green wave effect) of natural vegetation. Type III Final Report, NASA Goddard Space Flight Center, Green belt, Maryland.

Schaper, D. (2017). 3 reasons Houston was a 'sitting duck' for Harvey flooding. https://www.npr.org/2017/08/31/547575113/three-reasons-houston-was-a-sitting-duck-for-harvey-flooding. Accessed 5 June 2020.

Schiff, R., & Benoit, G. (2007). Effects of impervious cover at multiple spatial scales on coastal watershed streams. *Journal of the American Water Resources Association, 43*, 712–730.

Schueler, T. (2003). *Impacts of impervious cover on aquatic systems*, *Watershed protection research monograph no 1*. Ellicot City: Center for Watershed Protection.

Smil, V. (2000). Phosphorus in the environment: Natural flows and human interferences. *Annual Review of Energy and the Environment, 25*, 53–88.

Sridhar, B. B. M., & Gidudu, A. (2020). Effect of landscape changes on the water quality of Murchison Bay. *International Journal of Advanced Remote Sensing and GIS*. https://doi.org/10.23953/cloud.ijarsg.474.

Sridhar, B. B. M., Vincent, R. K., Witter, J. D., & Spongberg, A. L. (2009). Mapping the total phosphorus concentration of biosolid amended surface soils using LANDSAT TM data. *Science of the Total Environment, 407*, 2894–2899.

Sridhar, B. B. M., Vincent, R. K., Roberts, S. J., & Czajkowski, K. (2011). Remote sensing of soybean stress as an indicator of chemical concentration of biosolid amended surface soils. *International Journal of Applied Earth Observation, 13*, 676–681.

TCEQ. 1999. Chapter 350 – Texas risk reduction program. https://www.tceq.texas.gov/assets/public/legal/rules/rules/pdflib/350b.pdf. Accessed 5 June 2020.

TCEQ. 2014. 2014 Guidance for assessing and reporting surface water quality in Texas. https://www.tceq.texas.gov/assets/public/waterquality/swqm/assess/14txir/2014_guidance.pdf. Accessed 5 June 2020.

Theobald, D. M., Goetz, S. J., Norman, J. B., & Jantz, P. (2009). Watersheds at risk to increased impervious surface cover in the conterminous United States. *Journal of Hydrologic Engineering, 14*, 362–368.

Thronson, A., & Quigg, A. (2008). Fifty-five years of fish kills in coastal Texas. *Estuaries and Coasts, 31*(4), 802–813.

U.S.EPA. (2002). Summary table for the nutrient criteria documents. https://www.epa.gov/sites/production/files/2014-08/documents/criteria-nutrient-ecoregions-sumtable.pdf. Accessed 5 June 2020.

U.S.EPA. (2018). 2018 edition of the drinking water standards and health advisories. EPA 822-F-18-001. https://www.epa.gov/sites/production/files/2018-03/documents/dwtable2018.pdf. Accessed 5 June 2020.

UNDESA. 2018. World urbanization prospects: The 2018 revision. United Nations, Department of Economic and Social Affairs, Population Division. https://www.un.org/en/events/citiesday/assets/pdf/the_worlds_cities_in_2018_data_booklet.pdf. Accessed 5 June 2020.

USEPA. (1996). *Method 3050B: Acid Digestion of Sediments, Sludges, and Soils, Revision 2*. https://www.epa.gov/esam/epa-method-3050b-aciddigestion-sediments-sludges-and-soils. Accessed 5 June 2020.

USEPA. (2018). 2018 edition of the drinking water standards and health advisories. EPA 822-F-18-001. [Online]. [Accessed Feb 15, 2020]. Available from: https://www.epa.gov/sites/production/files/2018-03/documents/dwtable2018.pdf. Accessed 5 June 2020.

USNRC. (1999). *Arsenic in drinking water*. Washington, DC: United States National Research Council, National Academy Press. https://www.nap.edu/catalog/6444/arsenic-in-drinking-water. Accessed 5 June 2020.

Vincent, R. K., Qin, X., McKay, R. M. L., Miner, J., Czajkowski, K., Savino, J., & Bridgeman, T. (2004). Phycocyanin detection from LANDSAT TM data for mapping cyanobacterial blooms in Lake Erie. *Remote Sensing of Environment, 89*, 381–392.

Wasige, J. E., Groen, T. A., Smaling, E., & Jetten, V. (2013). Monitoring basin-scale land cover changes in Kagera Basin of Lake Victoria using ancillary data and remote sensing. *International Journal of Applied Earth Observation, 21*, 32–42.

WHO. (2011a). Arsenic in drinking water. WHO/SDE/WSH/03.04/75/Rev/1. https://www.who.int/water_sanitation_health/publications/arsenic/en/. Accessed 5 June 2020.

WHO. (2011b). Lead in drinking water. WHO/FWC/WSH/16.53. https://www.who.int/water_sanitation_health/water-quality/guidelines/chemicals/lead-background-feb17.pdf. Accessed 5 June 2020.

Wu, J., David, J. L., & Jenerette, G. D. (2003). Linking land use change with ecosystem processes: A hierarchical patch dynamics model. In S. S. Guhathakurta (Ed.), *Integrated Land Use and Environmental Models*. New York: Springer.

Yesilonis, I., Pouyat, R., & Neerchal, N. (2008). Spatial distribution of metals in soils in Baltimore, Maryland: Role of native parent material, proximity to major roads, housing age and screening guidelines. *Environmental Pollution, 156*, 723–731.